minerals

MDPI

Article

Application of Full Factorial Experimental Design and Response Surface Methodology for Chromite Beneficiation by Knelson Concentrator

Gul Akar Sen

Received: 17 November 2015; Accepted: 13 January 2016; Published: 19 January 2016
Academic Editor: Massimiliano Zanin

Department of Mining Engineering, Dokuz Eylul University, Buca 35370, Izmir, Turkey; gul.akar@deu.edu.tr; Tel.: +90-232-301-7537

Abstract: The present work is undertaken to determine the effect of operational variables, namely: feed rate, centrifugal force and fluidization water flow rate on the efficiency of Knelson concentrator for chromite ore beneficiation. A full factorial design with three factors at three levels and response surface methodology (RSM) were applied for this purpose. The quadratic models were developed to predict the concentrate Cr_2O_3 grade and recovery as the process responses. The results suggest that all the variables affect the grade and recovery of the Cr_2O_3 concentrate to some degree. However, the fluidization water rate was found as the most effective parameter.

Keywords: Knelson concentrator; chromite ores; gravity processing; full factorial design

1. Introduction

Chromite ore $(Mg,Fe)(Cr,Al,Fe)_2O_4$ is an oxide mineral which is the most important source of chromium. It is used for various purposes in metallurgical, refractory and chemical industries. In 2013, South Africa was the world's dominant chromite producer, followed by Kazakhstan, India and Turkey [1].

It is estimated that Turkey has about 31 million tons mineable reserves of high grade (30%–48% Cr_2O_3) chromite ore [2]. The type, amount and liberation conditions of the gangue minerals determine the mineral processing option. The redistribution of Cr_2O_3 to gangue minerals can lower the efficiency of the physical separation plants [3]. Different beneficiation techniques such as gravity separation [4–7], flotation [8–12] or magnetic separation [13–17] can be applied to remove gangue minerals from the chromite concentrates.

New generation gravity processing devices such as Mozley Multi Gravity Separator (MGS), Falcon Separator and Knelson Concentrator are promising technologies for the recovery of chromite at fine sizes. These gravity concentrators utilize centrifugal force to enhance the relative settling velocity between particles with different size and density [18–23].

The efficiency of centrifugal separators can be improved by adjusting the levels of operational parameters to provide the best conditions for separation [24,25]. For this reason, the effects of different operational parameters are crucial to understanding and controlling the separation process. However, it is very time consuming to test the whole set of parameters at all levels. For this reason, a well-designed experimental test program is needed to determine the response of the separation process to each factor. As of today, factorial designs have been used successfully in many different areas for planning of experiments to develop empirical models [26–29]. In this study, the effects of the operating variables such as feed rate, centrifugal force and fluidization water flow rate on the separation efficiency of Knelson concentrator were investigated using response surface methodology (RSM) and three-level and three-factor full factorial experimental design. Full factorial design contains

all possible combinations of a set of factors. The influences of all factors and interaction effects on the responses are investigated systematically.

2. Materials and Methods

2.1. Materials

The chromite ore used in the study was supplied from Adana, Turkey. Microscopic studies indicated harzburgite and dunite which are serpentinized to different degrees as the host rocks. The specific gravity of the ore sample was determined as 3.2 g/cm^3 using Micrometrics, Accupyc II 1340 Gas Pycnometer (Micromeritics Instrument Corporation, Norcross, GA, USA). The specific gravity of the chromite mineral is about 4.6 g/cm^3, whereas associated gangue minerals have a specific gravity of about 2.6 g/cm^3. These specific gravity values indicate that separation of these minerals from each other using a gravity concentration technique is possible.

The ore sample was stage-crushed to 100% below 3.35 mm and then ground to 100% below 500 µm using a laboratory rod mill. Wet sieve analysis was carried out to determine the particle size distribution of the ground material using a vibratory sieve shaker and micro precision sieves. The results of size-wise chemical analysis are presented in Table 1.

Table 1. Size-wise chemical analysis results of chromite.

Particle Size (µm)	Weight (%)	Grade (Cr_2O_3 %)	Distribution (Cr_2O_3 %)
500–300	5.0	17.0	3.4
300–212	5.7	20.1	4.6
212–150	8.1	20.3	6.6
150–106	7.7	24.8	7.7
106–75	10.6	32.0	13.6
75–53	11.0	32.2	14.2
53–38	11.1	31.9	14.2
−38	40.8	21.7	35.6
Total	100.0	24.9	100.0

2.2. Methods

A laboratory scale Knelson separator "KC-MD3" (FLSmidth USA Inc., Midvale, UT, USA) was used for the experiments. The concentrator has 45 kg/h dry and 8 L/min volumetric throughput. This manual discharge-laboratory scale separator has a 3 inches diameter truncated-cone-shaped separation bowl. The concentrate capacity of the separation bowl varies between 80 to 150 g depending on the fluidization conditions and heavy mineral properties. The amount of the feed material to be used in the study was determined as 220 g considering the chromite mineral content of the ore and results of the trial experiments. At the end of the study, the standard deviation of the weight of the concentrates was calculated as 1.8 g. The solid ratio of the feed slurry was kept constant 23% (*w*/*w*) during each test. The volumetric pulp flow rates corresponding to 12, 24 and 36 kg/h feed rates were 0.7, 1.4 and 2.2 L/min, respectively. The required fluidization water (FWFR) was supplied using a centrifugal pump with 4, 8 and 12 L/min flow rates.

The concentrate and tailing of the separation tests were filtered, dried and weighed prior to chemical analysis. Titration method (ASTM-E342-04, 1999) [30] was employed for the determination of the Cr_2O_3 content of different products.

The effect of different operating parameters on the separation efficiency of Knelson separator was investigated using a three-level three-factor full factorial experimental design approach. The list of the independent variables (*A*, *B*, *C*) with their coded and actual levels are presented in Table 2.

Table 2. Variables and levels for the three-level and three-factor full factorial design.

Variables	Symbol	Real Values of Coded Levels		
		−1	**0**	**+1**
Fluidization water flow rate ((FWFR), L/min)	*A*	4	8	12
G force	*B*	60	90	120
Feed rate (kg/h)	*C*	12	24	36

−1: factor at low level; 0: factor at medium level; +1: factor at high level.

A second order polynomial equation was chosen to fit the experimental results. This model represents the effects of process variables (A, B, C) and their interactions on the response variables (Cr_2O_3 grade and Cr_2O_3 recovery). The general form of the model chosen is represented as following:

$$Y = b_0 + b_1A + b_2B + b_3C + b_{12}AB + b_{13}AC + b_{23}BC + b_{11}A^2 + b_{22}B^2 + b_{33}C^2 \quad (1)$$

where, Y is the predicted response, b_0 is model constant; b_1, b_2 and b_3 are linear coefficients; b_{12}, b_{13} and b_{23} are cross product coefficients and b_{11}, b_{22} and b_{33} are the quadratic coefficients. Statistical Stat-Ease Design Expert 9.0.3.1 software (Stat-Ease Inc., Minneapolis, MN, USA) was used to establish the validity of the models on the basis of analysis of variance (ANOVA).

3. Results and Discussion

3.1. The Model Equations and Statistical Evaluation

A total of 32 tests including five control experiments (center points) were conducted during the experimental study. The actual data collected from the tests were used to construct the empirical models representing concentrate grade and recovery as process responds to the variables. The results obtained from the tests are presented in Table 3.

Table 3. Design matrix and the results of the three-level and three-factor factor full factorial design.

Run Number	Conditions			Grade, Cr_2O_3 %		Recovery, Cr_2O_3 %	
	A	***B***	***C***	**Actual**	**Predicted**	**Actual**	**Predicted**
1	12	60	24	42.3	42.8	68.1	68.7
2	12	90	24	41.3	40.1	70.8	69.4
3	8	90	24	37.9	37.6	66.1	66.8
4	8	90	24	36.5	37.6	64.7	66.8
5	12	90	12	40.3	39.9	71.7	71.9
6	4	60	12	33.3	33.6	61.0	61.8
7	4	90	36	30.3	30.1	53.2	54.6
8	12	120	12	37.0	37.4	71.9	71.8
9	12	120	24	37.8	37.8	68.5	69.2
10	4	120	36	28.2	28.3	50.3	49.4
11	4	120	12	29.1	28.8	52.9	52.4
12	4	60	36	32.2	32.2	59.7	59.0
13	4	90	24	30.0	30.4	54.4	55.3
14	8	90	24	37.1	37.6	66.4	66.8
15	8	120	36	35.5	35.8	63.2	63.3
16	8	120	24	35.7	35.5	64.2	64.2
17	8	90	12	38.8	37.9	69.9	69.2
18	8	60	36	40.5	40.0	67.2	67.9
19	4	90	12	30.6	31.0	57.2	57.5
20	12	60	12	42.2	42.8	70.9	71.1
21	8	60	24	40.9	40.1	68.6	68.7
22	8	60	12	41.2	40.6	71.5	71.0

Table 3. *Cont.*

Run Number	Conditions			Grade, Cr_2O_3 %		Recovery, Cr_2O_3 %	
	A	*B*	*C*	Actual	Predicted	Actual	Predicted
23	12	120	36	38.5	38.5	68.0	68.2
24	8	90	24	36.9	37.6	68.0	66.8
25	12	90	36	41.1	40.7	69.0	68.4
26	8	120	12	34.9	35.5	66.1	66.6
27	4	120	24	29.2	28.4	50.1	50.1
28	8	90	24	37.9	37.6	66.9	66.8
29	8	90	24	37.5	37.6	68.6	66.8
30	8	90	36	37.5	37.7	66.6	66.0
31	12	60	36	42.7	43.1	67.7	67.8
32	4	60	24	32.8	32.7	60.9	59.6

Table 3 also shows the predicted responses of the process to the variables considered. The actual model equation for grade (Y_1) and recovery (Y_2) of the chromite concentrates is given in Equations (2) and (3) respectively.

$$Y_1 = 37.64 + 4.86A - 2.34B - 0.057C - 0.16AB + 0.41AC + 0.20BC - 2.37A^2 + 0.16B^2 + 0.16C^2 \quad (2)$$

$$Y_2 = 66.83 + 7.05A - 2.25B - 1.58C + 2.51AB - 0.15AC - 0.057BC - 4.51A^2 - 0.42B^2 + 0.78C^2 \quad (3)$$

The models fit the data well and the differences between the observed values and the model's predicted values are relatively small and unbiased. The predicted values are in consistent with the experimental results. The coefficients of determination (R^2) obtained for the grade and recovery are 0.9852 and 0.9830 respectively, indicating that the regression is significant as illustrated in Figure 1.

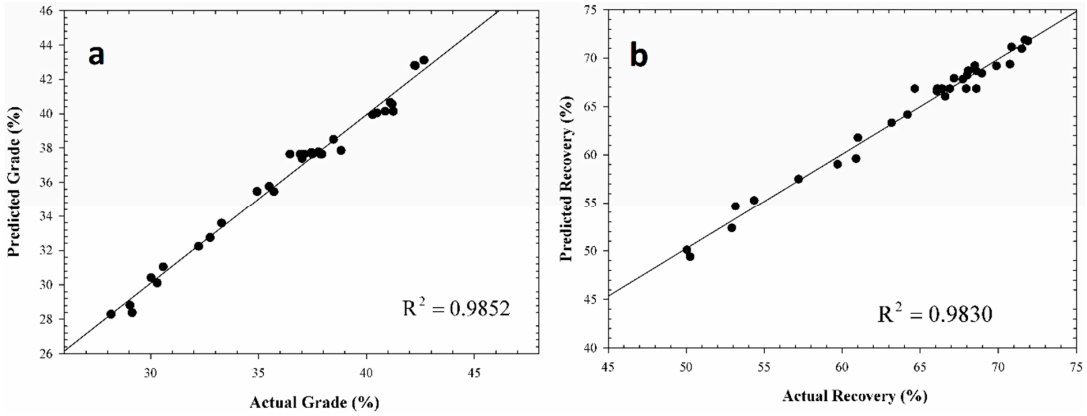

Figure 1. Relationship between observed and predicted values ((**a**) Grade; (**b**) Recovery).

Figure 2 shows graphically the residuals for predicted values of grade and recovery. As can be seen from these figures that the residual values are uniformly distributed.

The significance test of model fit for grade and recovery of the concentrates were performed using Design Expert software version 9.0.3.1 based on analysis of variance (ANOVA). The results showed that the models are significant as the *F* value is high and the Prob > *F* value is less than 0.05 (Table 4). The standard deviations of the predicted models were found 0.62 and 1.0 for grade and recovery respectively. Lack of Fit *F*-values were found as 1.23 for grade and 0.36 for recovery models implying that the Lack of Fit is not significant relative to the pure error for both models. The predicted R^2 values of grade and recovery models (0.9714 and 0.9678 respectively) are in reasonable consistency with the

adjusted R^2 values (0.9791 and 0.9761), the difference between these two values are less than 0.2 for both models.

The significance level of the parameters, the coefficient estimates and parameter interactions of the empirical models are tabulated in Table 5. Values of "Prob > *F*" less than 0.05 for the models suggest that the model terms are significant.

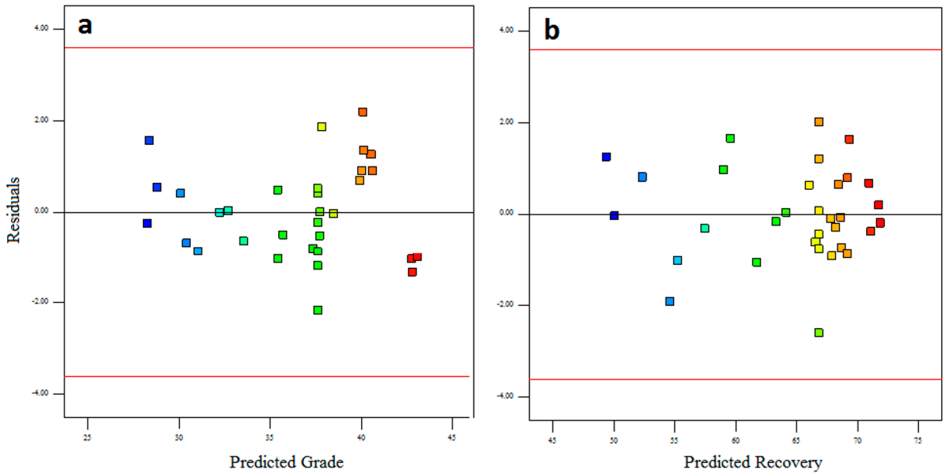

Figure 2. Residual plots for predicted grade and recovery values ((**a**) Grade; (**b**) Recovery).

Table 4. Analysis of variance (ANOVA) table derived for the grade and recovery models.

Statistics	Source	
	Cr_2O_3 (%) Grade Model	Cr_2O_3 (%) Recovery Model
Sum of square	569.35	1265.55
Degree of freedom	9	9
Mean square	63.26	140.62
F-Value	162.72	141.39
Prob > *F*	<0.0001	<0.0001
Standard deviation	0.62	1.00
Adjusted R^2	0.9791	0.9761
Predicted R^2	0.9714	0.9678
R^2	0.9852	0.9830

Table 5. Estimated coefficient values for the parameter and parameter interaction effects.

Factor	Cr_2O_3 (%) Grade			Cr_2O_3 (%) Recovery		
	Coefficient Estimate	*F*-Value	Prob > *F*	Coefficient Estimate	*F*-Value	Prob > *F*
A—FWFR	4.86	1095.08	<0.0001	07.05	899.85	<0.0001
B—G Force	−2.34	254.362	<0.0001	−2.25	91.40	<0.0001
C—Feed	−0.057	0.145	0.70	−1.58	44.96	<0.0001
AB	−0.16	0.83	0.37	2.51	75.97	<0.0001
AC	0.41	5.21	0.03	−0.15	0.27	0.6115
BC	0.20	1.28	0.27	−0.057	0.04	0.8435
A^2	−2.37	103.18	<0.0001	−4.51	146.43	<0.0001
B^2	0.16	0.45	0.51	−0.42	1.27	0.2719
C^2	0.16	0.48	0.49	0.78	4.41	0.0474

3.2. The Effect of Process Variables on Grade of the Knelson Separator Concentrate

The estimated coefficient values calculated for main effects of the process variables from the Equation 2 (Table 5) indicate that fluidization water flow rate (*A*) has a positive effect and *G* force (*B*)

has a negative effect on the Cr_2O_3 content of the concentrate. It was also observed that feed rate (*C*) has no significant effect on the grade of the concentrate in the range of the parameter levels tested.

The Equation 2 dictates that the interaction of variables, fluidization water flow rate (*A*)—*G* force (*B*) has a negative effect on the Cr_2O_3 content of the concentrate whereas interactions of fluidization water flow rate (*A*)—feed rate (*C*) and *G* force (*B*)—feed rate (*C*) have a positive effect. On the other hand, fluidization water flow rate (*A*) has the highest quadratic effect on the concentrate Cr_2O_3 grade.

The predicted response (Y_1) of the process to the independent variables are presented graphically in three dimensional (3D) space to help to visualize the shape of the response surface in Figures 3–5.

The effect of the *G* force and fluidization water flow rate on grade (Cr_2O_3 %) of the concentrate at the center level of feed rate is shown in Figure 3. As can be seen from Figure 3, a higher grade concentrate is obtained at higher fluidization water flow rate and at lower *G* force. The grade of the concentrate tends to decrease as the applied *G* force increases. This can be explained by the fact that the cut-density of the separation is reduced with increasing *G* force which in turn allows the lower grade composite particles to enter the concentrate product and decrease the Cr_2O_3 grade.

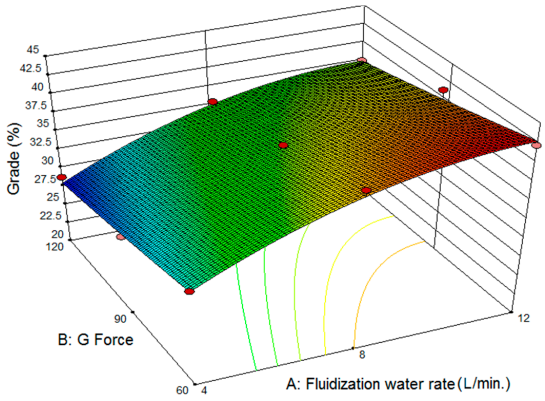

Figure 3. The response surface plot representing the effect of fluidization water flow rate and applied *G* force on the Cr_2O_3 content of the concentrate.

Figure 4 illustrates the effect of feed rate and fluidization water flow rate on grade (Cr_2O_3 %) of the concentrate at the center level of *G* force. It is seen from Figure 4 that there is not any significant effect of feed rate on the grade of the concentrate at a constant water flow rate in the range of the parameter levels tested. However, increasing the fluidization water flow rate leads to obtaining higher grade concentrate due to the increased number of light particles transported to the outside of separation cone.

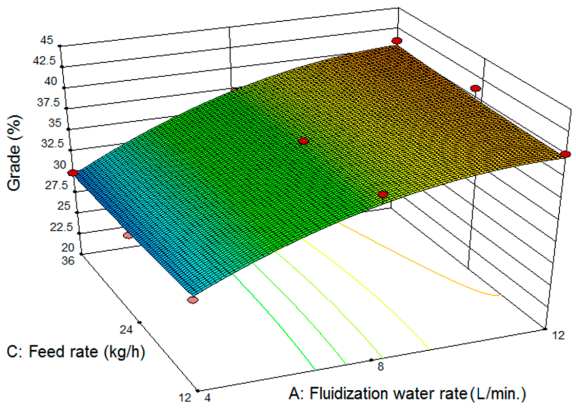

Figure 4. The response surface plot representing the effect of fluidization water flow rate and feed rate on the Cr_2O_3 content of the concentrate.

Figure 5 represents the effect of *G* force and feed rate on grade (Cr_2O_3 %) of the Knelson concentrate at the center level of fluidization water flow rate. It is observed from Figure 5 that changing feed rate has no significant effect on the concentrate grade in the range of the parameter levels tested. On the other hand, the use of higher *G* force at a constant feed rate results in a decrease in concentrate Cr_2O_3 grade.

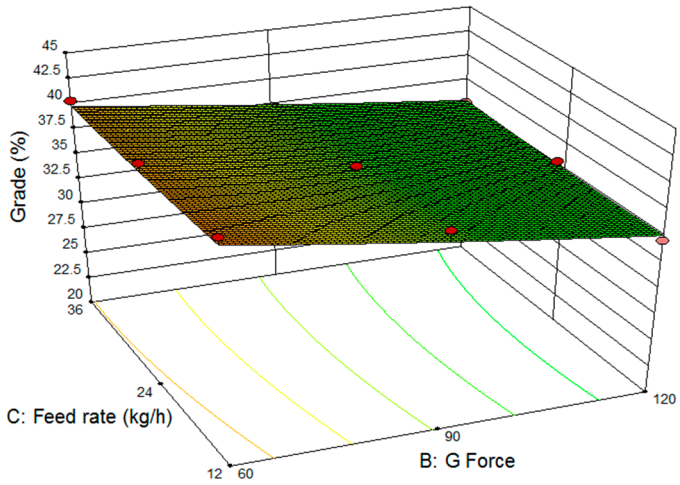

Figure 5. The response surface plot representing the effect of *G* force and feed rate on the Cr_2O_3 content of the concentrate.

3.3. Effect of KC-MD3 Knelson Concentrator Variables on Concentrate Recovery

The estimated coefficient and Prob > *F* values obtained for main effects of the independent variables from Equation 3 indicate that water flow rate (*A*) has a positive effect on the Cr_2O_3 recovery of the concentrate, whereas, *G* force (*B*) and feed rate (*C*) negatively affect the Cr_2O_3 recovery.

The interaction of variables fluidization water flow rate (*A*)—*G* force (B) has a significant positive effect on the Cr_2O_3 recovery of the concentrate, while interactions of fluidization water flow rate (*A*)—feed rate (*C*) and *G* force (*B*)—feed rate (*C*) have a negative effect. It is also important to note that fluidization water flow rate (*A*) has a significant quadratic effect on the concentrate Cr_2O_3 recovery compared to the other independent variables.

Figure 6 illustrates the effect of *G* force and fluidization water flow rate on the recovery of Cr_2O_3 in the Knelson concentrate. Feed rate was kept constant at the center level during this test. At low level of fluidization water rate, as the *G* force increases, recovery of Cr_2O_3 decreases significantly due to inefficient fluidization of the separation layer inside the bowl. The highest recovery value was obtained by increasing fluidization water level to maximum for providing the appropriate conditions of fluidization.

Figure 7 shows the effect of fluidization water flow rate and feed rate on recovery of Cr_2O_3 in the concentrate of Knelson separator at the center level of *G* force. As can be seen from Figure 7, increasing fluidization water rate provides better fluidization conditions in the separation layer and helps to increase Cr_2O_3 recovery of concentrate. It should be noted that there is a significant decrease in the recovery of Cr_2O_3 at high feed rate when the fluidization water rate is low.

Figure 8 demonstrates the effect of feed rate and *G* force on Cr_2O_3 recovery of the concentrate at the center level of fluidization water flow rate. As the *G* force decreases the transport of the lighter particles to the tailing fraction degreases which in increases recovery of Cr_2O_3 to the concentrate fraction.

Figure 8 was plotted representing the recovery of Cr_2O_3 concentrate *vs.* feed rate and *G* force. The Cr_2O_3 recovery of the concentrate increases with decrease in feed rate and *G* force. The lowest level of both independent variables appears to be providing favorable conditions for an efficient separation at

this level of fluidization water flow. Increasing any of these variables to a higher level seems to change the fluidization conditions and lower the Cr_2O_3 recovery due to the disruption of the separation layer.

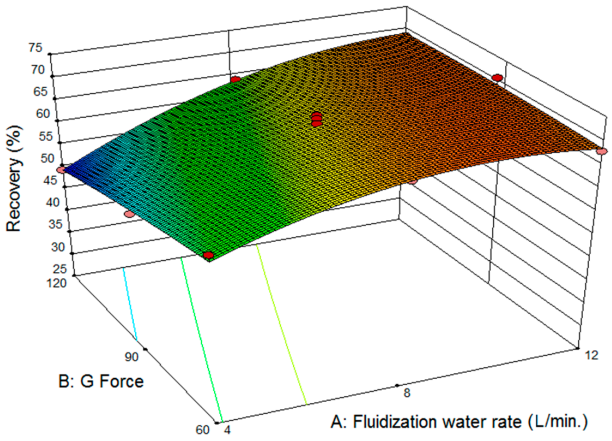

Figure 6. The response surface plot representing the effect of fluidization water flow rate and applied *G* force on the Cr_2O_3 recovery of the concentrate.

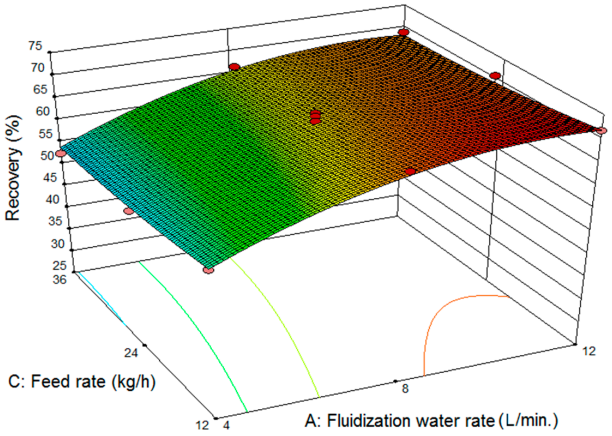

Figure 7. The response surface plot representing the effect of fluidization water flow rate and feed rate on the Cr_2O_3 recovery of the concentrate.

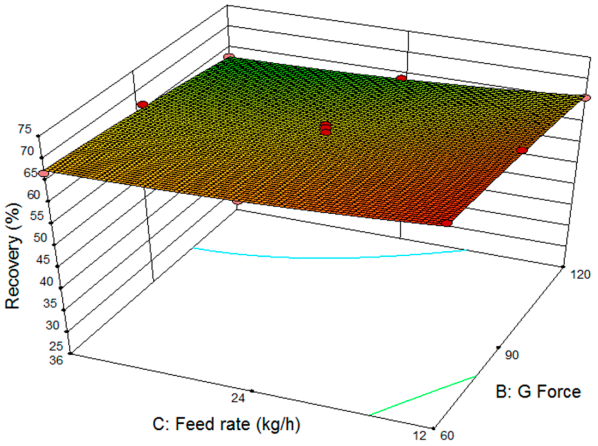

Figure 8. The response surface plot representing the effect of *G* force and feed rate on the Cr_2O_3 recovery of the concentrate.

3.4. Validation of the Models

For validation of the obtained models for predicting the grade and recovery of Cr_2O_3 content in concentrate, nine additional tests were conducted using different levels of independent variables. The test conditions and results are presented in Table 6.

Table 6. The conditions and actual and predicted results of the validation tests.

Run Number	Conditions			Grade, Cr_2O_3 %		Recovery, Cr_2O_3 %	
	A	*B*	*C*	Actual	Predicted	Actual	Predicted
1	4	60	18	31.8	33.1	57.5	60.5
2	8			41.3	40.3	72.7	69.6
3	12			41.8	42.8	69.1	69.7
4	4	90		29.5	30.7	53.0	56.2
5	8			37.6	37.7	68.7	67.8
6	12			40.5	40.0	72.6	70.4
7	4	120		28.7	28.6	50.8	51.0
8	8			35.1	35.4	64.5	65.2
9	12			41.1	37.5	72.3	70.3

The observed results and the predicted results for both responses are illustrated in Figure 9. Figure 9 shows that the predicted values are consistent with the observed values, with R^2 of 0.9254 percent for grade and R^2 of 0.9635 percent for recovery of chromite concentrates.

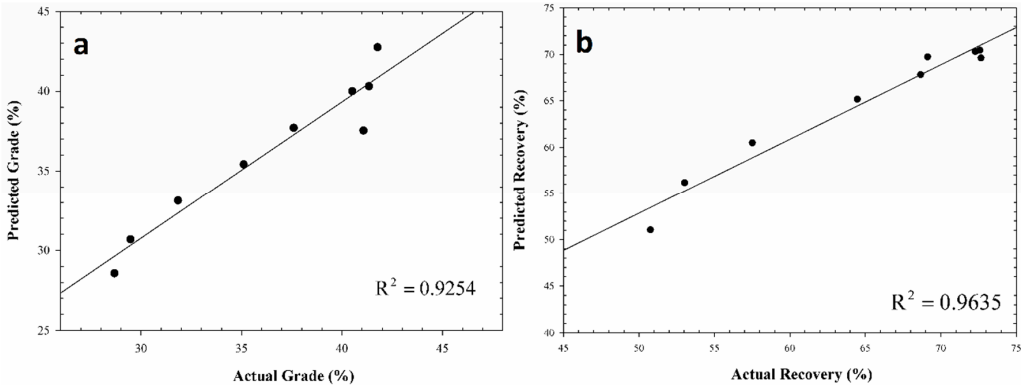

Figure 9. Relationship between actual and predicted results of the validation tests. ((**a**) Grade; (**b**) Recovery)

3.5. Optimization

The optimized independent variable levels for making the grade and recovery values maximum were also determined using the optimization module of Design Expert version 9.0.3.1. The numerical optimization option of the module was utilized by employing the developed models to search the factor space for the best trade-offs to achieve the highest grade and recovery in the range of the experimental data. The results showed that a concentrate assaying 43% Cr_2O_3 with 72% Cr_2O_3 recovery can be obtained by adjusting the variables to the following levels; fluidization water rate of 11 L/min, *G* force of 60 G, feed rate of 12 kg/h.

4. Conclusions

In this study, the effect of feed rate (kg/h), *G* force and fluidization water flow rate (L/min) on the chromite beneficiation process by KC-MD3 Knelson concentrator was investigated. Full factorial experimental design and response surface methodology were used to develop mathematical models

for both grade and recovery of Cr_2O_3 concentrate. Mathematical model equations were derived using experimental data and mathematical software package Design Expert 9.0.3.1. It was found that the predicted values were in reasonable consistency with the experimental data which were also confirmed by the validation experiments. The ANOVA results indicated that fluidization water flow rate was the dominant independent variable affecting both grade and recovery of the concentrate. The results of the numerical optimization in the range of the experimental data showed that it is possible to produce a concentrate assaying 43% Cr_2O_3 with 72% Cr_2O_3 recovery by operating Knelson concentrator at the fluidization water rate of 11 L/min, *G* force of 60 G and feed rate of 12 kg/h.

Conflicts of Interest: The authors declare no conflict of interest.

References

1. U.S. Geological Survey. Mineral Commodity Summaries. Available online: http://minerals.usgs.gov/minerals/pubs/mcs/2015/mcs2015.pdf (accessed on 8 November 2015).
2. Cicek, T.; Cocen, I.; Engin, V.T.; Cengizler, H.; Sen, S. Technical and economical applicability study of centrifugal force gravity separator (MGS) to Kef chromite concentration plant. *Miner. Process. Extr. Metall.* **2008**, *117*, 248–255. [CrossRef]
3. Grieco, G.; Pedrotti, M.; Moroni, M. Metamorphic redistribution of Cr within chromitites and its influence on chromite ore enrichment. *Miner. Eng.* **2011**, *24*, 102–107. [CrossRef]
4. Kapure, G.; Kari, C.; Rao, S.M.; Rao, N.D. The feasibility of a slip velocity model for predicting the enrichment of chromite in a Floatex density separator. *Int. J. Miner. Process.* **2007**, *82*, 86–95. [CrossRef]
5. Kumar, C.R.; Tripathy, S.K.; Rao, D.S. Characterisation and pre-concentration of chromite values from plant tailings using floatex density separator. *J. Miner. Mater. Charact. Eng.* **2009**, *8*, 367–378. [CrossRef]
6. Tripathy, S.K.; Ramamurthy, Y.; Singh, V. Recovery of chromite values from plant tailings by gravity concentration. *J. Miner. Mater. Charact. Eng.* **2011**, *10*, 13–25. [CrossRef]
7. Tripathy, S.K.; Ramamurthy, Y. Modeling and optimization of spiral concentrator for separation of ultrafine chromite. *Powder Technol.* **2012**, *221*, 387–394. [CrossRef]
8. Guney, A.; Onal, G.; Celik, M.S. A new flowsheet for processing chromite fines by column flotation and the collector adsorption mechanism. *Miner. Eng.* **1999**, *12*, 1041–1049. [CrossRef]
9. Feng, D.; Aldrich, C. Adsorption of heavy metals by biomaterials derived from the marine alga Ecklonia maxima. *Hydrometallurgy* **2004**, *73*, 1–10. [CrossRef]
10. Gallios, G.P.; Deliyanni, E.A.; Pelek, E.N.; Matis, K.A. Flotation of chromite and serpentine. *Sep. Purif. Technol.* **2007**, *55*, 232–237. [CrossRef]
11. Smith, R.W.; Allards, S.G. Effects of pretreatment and aging on chromite flotation. *Int. J. Miner. Process.* **1983**, *11*, 163–174. [CrossRef]
12. Sysila, S.; Laapas, H.; Heiskanen, K.; Ruokonen, E. The effect of surface potential on the flotation of chromite. *Miner. Eng.* **1996**, *9*, 519–525. [CrossRef]
13. Aslan, N.; Kaya, H. Beneficiation of chromite concentration waste by multi-gravity separator and high intensity induced-roll magnetic separator. *Arab. J. Sci. Eng.* **2009**, *34*, 285–297.
14. Tripathy, S.K.; Murthy, Y.R.; Singh, V. Characterisation and separation studies of Indian chromite beneficiation plant tailing. *Int. J. Miner. Process.* **2013**, *122*, 47–53. [CrossRef]
15. Ucbas, Y.; Bozkurt, T.V.; Bilir, K.; Ipek, H. Separation of chromite from serpentine in fine sizes using magnetic carrier. *Sep. Purif. Technol.* **2014**, *49*, 946–956. [CrossRef]
16. Ucbas, Y.; Bozkurt, T.V.; Bilir, K.; Ipek, H. Concentration of chromite by means of magnetic carrier using sodium oleate and other reagents. *Physicochem. Probl. Miner. Process.* **2014**, *50*, 767–782.
17. Tripathy, S.K.; Banerjee, P.K.; Suresh, N. Magnetic separation studies on ferruginous chromite fine to enhance Cr:Fe ratio. *Int. J. Miner. Metall. Mater.* **2015**, *22*, 217–224. [CrossRef]
18. Gence, N. Beneficiation of Elazığ-Kefdağı chromite by multi-gravity separator. *Turk. J. Eng. Environ. Sci.* **1993**, *23*, 473–475.
19. Knelson, B.; ve Jones, R. A new generation of Knelson concentrators a totally secure system goes on line. *Miner. Eng.* **1993**, *7*, 201–207. [CrossRef]

20. Guney, A.; Önal, G.; Atmaca, T. New aspect of chromite gravity tailings re-processing. *Miner. Eng.* **2001**, *14*, 1527–1530. [CrossRef]
21. Sen, S. Gold recovery by KC from grinding circuit of Bergama CIP plant. *Rem Rev. Esc. Minas* **2010**, *63*, 539–545. [CrossRef]
22. Uslu, T.; Sahinoglu, E.; Yavuz, M. Desulphurization and deashing of oxidized fine coal by Knelson concentrator. *Fuel Process. Technol.* **2012**, *101*, 94–100. [CrossRef]
23. Kökkılıç, O.; Langlois, R.; Waters, K.E. A design of experiments investigation into dry separation using a Knelson concentrator. *Miner. Eng.* **2015**, *72*, 73–86. [CrossRef]
24. Aslan, N. Multi-objective optimization of some process parameters of a multi-gravity separator for chromite concentration. *Sep. Purif. Technol.* **2008**, *64*, 237–241. [CrossRef]
25. Altun, N.E.; Sakuhuni, G.; Klein, B. The use of continuous centrifugal gravity concentration in grinding circuit. Modified approach for improved metallurgical performance and reduced grinding requirements. *Physicochem. Probl. Miner. Process.* **2015**, *51*, 115–126.
26. Obeng, D.P.; Morrell, T.S.; Napier-Munn, T.J. Application of central composite rotatable design to modelling the effect of some operating variables on the performance of the three-product cyclone. *Int. J. Miner. Process.* **2005**, *76*, 181–192. [CrossRef]
27. Dehghan, R.; Noaparast, M.; Kolahdoozan, M.; Mousavi, S.M. Statistical evaluation and optimization of factors affecting the leaching performance of a sphalerite concentrate. *Int. J. Miner. Process.* **2008**, *89*, 9–16. [CrossRef]
28. Sharma, S.; Sharma, N.; Gupta, G.D. Optimizing of promethazine theoclate fast dissolving tablet using pore forming technology by 3-factor, 3-level response surface-full factorial design. *Arch. Pharm. Res.* **2010**, *33*, 1199–1207. [CrossRef] [PubMed]
29. Martinez, A.L.; Uribe, A.S.; Carrillo, F.R.P.; Coreno, J.A.; Ortiza, J.C. Study of celestite flotation efficiency using sodium dodecyl sulfonate collector: Factorial experiment and statistical analysis of data. *Int. J. Miner. Process.* **2003**, *70*, 83–97. [CrossRef]
30. ASTM, E342-04. *Standard Test Method for Determination of Chromium Oxide in Chrome Ores by Permanganate Titrimetry*; American Society for Testing and Materials (ASTM): West Conshohocken, PA, USA, 1999.